

## Mastering the Molecular Dynamics of a Bistable Molecule by Single Atom Manipulation

M. Martin,<sup>1</sup> M. Lastapis,<sup>1</sup> D. Riedel,<sup>1</sup> G. Dujardin,<sup>1</sup> M. Mamatkulov,<sup>2</sup> L. Stauffer,<sup>2</sup> and Ph. Sonnet<sup>2</sup>

<sup>1</sup>Laboratoire de Photophysique Moléculaire, Bâtiment 210, Université Paris Sud, 91405 Orsay Cedex, France

<sup>2</sup>Laboratoire de Physique et de Spectroscopie électronique, Université de Haute Alsace-CNRS UMR 7014, 4, rue des Frères Lumière, 68093 Mulhouse Cedex, France

(Received 5 April 2006; published 21 November 2006)

At low temperature (5 K), a single biphenyl molecule adsorbed on a Si(100) surface behaves as a bistable device which can be reversibly switched by electronic excitation with the scanning tunneling microscope tip. Density functional theory suggests that the biphenyl molecule is adsorbed with one dissociated hydrogen atom bonded to a neighbor surface silicon atom. By desorbing this hydrogen atom with the STM tip, the interaction of the molecule with the surface is modified such that it becomes transformed into a multistable device with four stable states having switching yields increased by almost 2 orders of magnitude.

DOI: 10.1103/PhysRevLett.97.216103

PACS numbers: 68.37.Ef, 68.35.Ja, 68.43.-h, 82.37.Gk

The operation of a single molecule as a molecular nanomachine requires controlling the interaction between the molecule and its surroundings with an atomic-scale precision [1–8]. This has been anticipated by Di Ventra *et al.* [9] from a theoretical viewpoint in calculating the electron transport properties through a molecule. The presence of a single gold atom at the molecule-electrode interface has been shown to decrease the molecular conductance by 2 orders of magnitude. Not only the conductance but other molecular functions (i.e., mechanical or chemical) are also expected to be very sensitive to the atomic-scale environment. Recently, it has been demonstrated that a single biphenyl molecule adsorbed on a Si(100) surface behaves as a bistable molecule at low temperature (5 K) via tip electrons [10]. The underlying physics describing the dynamics of such a molecular device is governed by a multi-dimensional surface potential that should be subtly influenced by the interaction between the molecule and its atomic-scale surroundings.

In this Letter, we will show that density functional theory (DFT) enables a precise map of the adsorption configuration of the biphenyl molecule. During its adsorption on Si(100), one hydrogen atom dissociates from one phenyl ring and bonds to a neighbor surface silicon atom. We will show that, after desorbing this hydrogen atom with the STM tip, the dynamics of the adsorbed biphenyl molecule is strongly modified. The stability of the molecule is affected such that it becomes a multistable molecule having four stable states. Moreover, the switching yields are increased by almost 2 orders of magnitude. These results demonstrate that single atom manipulation can be used to modify the dynamical properties of a single molecule.

The STM experiments were performed in an ultrahigh vacuum (UHV) chamber using a low temperature “beetle” type scanning tunneling microscope [11]. The Si(100) samples were *p*-type boron doped with a resistivity of 0.004–0.006  $\Omega$  cm. The Si(100) surface was prepared and cleaned as explained elsewhere [11]. The biphenyl molecules were adsorbed on the Si(100) surface at room

temperature [12]. The sample was then cooled down to 5 K and transferred into the UHV low temperature (5 K) STM.

STM topographies of biphenyl molecules adsorbed on the Si(100) surface are shown in Figs. 1(a) and 1(b) for a surface voltage of  $-2$  and  $-1$  V, respectively. STM topographies of a single biphenyl molecule are shown in Figs. 1(c) and 1(d). For a surface voltage of  $-2$  V [Figs. 1(a) and 1(c)], each biphenyl molecule is seen as a pair of bright features representing the two phenyl rings of the molecule. The vertical gray lines in Figs. 1(a)–1(d) indicate the silicon dimer rows of the Si(100) surface [11]. Only one of the two phenyl rings is visible as a bright spot for a surface voltage of  $-1$  V [Figs. 1(b) and 1(d)]. A variety of configurations for the adsorbed biphenyl molecule were investigated by means of DFT calculations within the generalized gradient approximation using the VASP code [13–15]. Further information on these calculations can be found elsewhere [16]. The resulting most stable configuration is shown in Figs. 1(g) and 1(h). Local density of states calculations, using the Tersoff-Hamann approximation [17], integrated over a window of energies from  $-2$  and  $-1$  eV to the Fermi level of this model were then performed and compared to the experimental STM topographies. The corresponding images are displayed in Figs. 1(e) and 1(f). The model consists of one phenyl ring lying parallel to the surface and attached to a silicon dimer in the so-called “butterfly” configuration through two C-Si chemical bonds [18]. This phenyl ring is centered over the silicon dimer row. The second phenyl ring, perpendicular to the surface, is attached to a silicon atom through a single C-Si chemical bond. This is a result of the dissociation of the second phenyl ring and one hydrogen atom: The H atom of the phenyl ring is bonded to the Si atom of the dimer as shown in Figs. 1(g) and 1(h). In the hypothesis of a nondissociated biphenyl molecule, less energetically favorable configurations were obtained and the simulations could not reproduce the observed STM topographies. This Si-H bond is seen as a dark spot in the STM topographies [Figs. 1(c) and 1(d)]. Interestingly, the

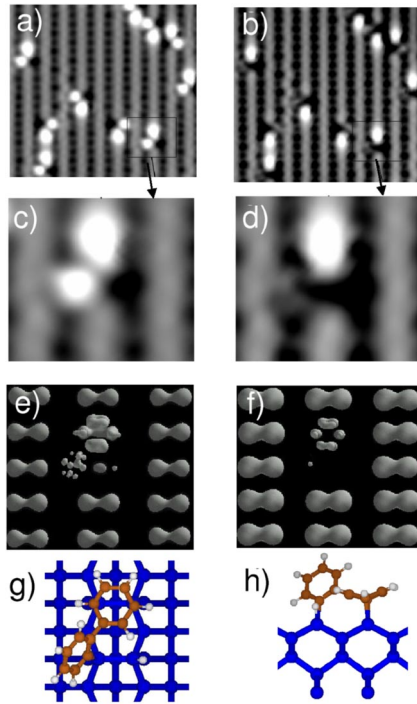


FIG. 1 (color online). (a),(b) ( $81 \text{ \AA} \times 75 \text{ \AA}$ ) STM topographies showing several biphenyl molecules on Si(100)-(2  $\times$  1) at 5 K recorded at  $-2$  and  $-1$  V surface voltage, respectively. (c),(d)  $19 \text{ \AA} \times 19 \text{ \AA}$  enlarged STM topographies of a biphenyl molecule on Si(100)-(2  $\times$  1) at  $V_S = -2$  V and  $V_S = -1$  V, respectively. (e),(f) Calculated local density of states (VASP) of a biphenyl molecule adsorbed on Si(100)-(2  $\times$  1) within an energy windows of  $-2$  and  $-1$  eV to the Fermi levels, respectively. (g) Schematic top view and (h) right-side view of the biphenyl conformation on the Si(100)-(2  $\times$  1) surface where the dark gray balls are silicon, the light gray balls are carbons atoms, and the white balls are the hydrogen atoms.

bright spot of the singly bound phenyl ring vanishes at  $V_S = -1$  V in both the experimental topography [Fig. 1(d)] and the calculated local density of states [Fig. 1(f)].

The biphenyl molecule adsorbed at room temperature on the Si(100) surface has two equivalent stable positions  $S_1$  and  $S_2$ , shown in Figs. 2(a) and 2(b), respectively. The reversible switching of the molecule from  $S_1$  to  $S_2$  can be activated through resonant electronic excitation by positioning the STM tip at different positions inside the molecule [for example, positions  $P_1$  and  $P_2$  in Fig. 2(a)] and applying a pulse voltage on the surface [10]. Recording the tunnel current during the pulse voltage enables a detailed investigation of the dynamics of the molecule for the duration of the time of excitation. The tunnel current curves in Figs. 2(c)–2(e), recorded with the STM tip in position  $P_2$ , illustrate some of the molecular movements that can occur. The small steps in curves 2(c) and 2(d) correspond to the switching of the molecule from  $S_1$  to  $S_2$ . The tunnel current curves show additional features consisting of very narrow peaks ( $T$ ) that are related to the brief passage through a transient molecular state, i.e., the  $S_1 \rightarrow T$

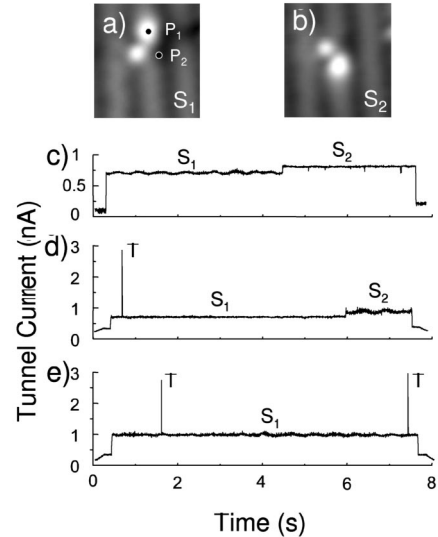


FIG. 2. (a) ( $23 \text{ \AA} \times 23 \text{ \AA}$ ) topography ( $V_S = -2$  V,  $I = 220$  pA) of a single biphenyl molecule in the stable configuration  $S_1$ . The dots indicate the STM tip position ( $P_1$  and  $P_2$ ) where the negative bias pulse is applied. (b) Same as (a) after the surface pulse. The molecule has switched to its second stable configuration  $S_2$ . (c)–(e) Three typical tunnel current curves recorded during negative bias pulses at  $P_2$  ( $V_S = -3$  V).

movement rapidly followed by the reverse  $T \rightarrow S_1$  movement. Both the  $S_1 \rightarrow T$  and the  $T \rightarrow S_1$  movements are induced by electronic excitation with the STM tip. From previous experiments [10] and the high tunnel current of the  $T$  peaks, one can anticipate that the  $T$  state molecular configuration involves one phenyl ring of the molecule being close to the  $P_2$  position in Fig. 2(a). This explains the very efficient excitation of the reverse  $T \rightarrow S_1$  movement when the STM tip is in the  $P_2$  position. The biphenyl molecule could never be imaged in the transient  $T$  state with the STM due to the instability either intrinsic to the molecule or induced by the STM tip.

The  $S_1 \rightarrow S_2$  switching requires one of the molecular phenyl rings (called the mobile phenyl ring) to break two Si-C bonds in its butterfly position, to move over the Si-H bond, and to make two new Si-C bonds to recover its butterfly position at the second silicon dimer site. In the meantime, the other molecular phenyl ring (called the fixed phenyl ring) is expected to rotate around its single Si-C bond. It follows that the Si-H bond acts as an obstacle to the movement of the bistable molecule since the mobile ring has to pass over the hydrogen atom for  $S_1 \rightarrow S_2$  switching to occur. Therefore, we decided to desorb this hydrogen atom with the STM tip in order to explore the resulting dynamics of the molecule.

The desorption of hydrogen atoms from the hydrogenated Si(100) surface with the STM tip has been extensively studied with both positive and negative surface voltages [19–22]. Here we have used a negative surface voltage  $V_S = -4$  V with the STM tip on top of the hydrogen atom [position  $P_2$  in Fig. 2(a)]. The desorption of the hydrogen atom after an excitation time  $t_d$  is clearly evident in the

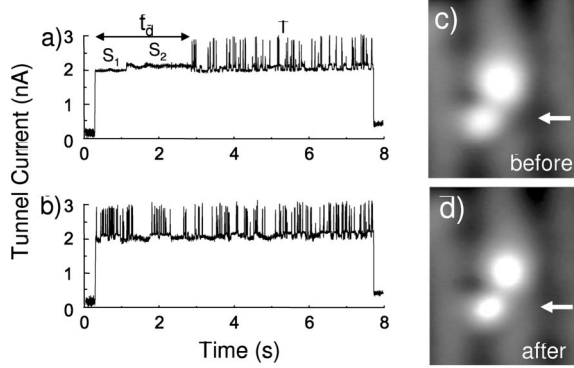


FIG. 3. (a) Tunnel current during a negative bias pulse at  $P_2$  ( $V_s = -4$  V). Desorption of the hydrogen atom occurs at time  $t_d$ . (b) Tunnel current during a negative bias pulse ( $V_s = -4$  V) after hydrogen desorption. (c),(d)  $20 \text{ \AA} \times 20 \text{ \AA}$  STM topographies ( $V_s = -2$  V,  $I = 220$  pA) of the biphenyl molecule before and after the hydrogen desorption. The arrow indicates the area where the hydrogen atom has been removed leading to a slightly higher local density of states. See Fig. 2 for the description of positions  $P_1$  and  $P_2$ .

tunnel current curve in Fig. 3(a). Indeed, before time  $t_d$ , the molecule switches only once from  $S_1$  to  $S_2$ . After a time  $t_d$ , the molecule has a completely different behavior. It switches much more often between the  $S_1$ ,  $S_2$ , and  $T$  states. This change has been found to be irreversible since the high frequency switching regime remains even after further surface voltage pulses applied at  $P_2$  [see Fig. 3(b)]. The actual desorption of the hydrogen atom can be verified by comparing STM topographies of the biphenyl molecule before [Fig. 3(c)] and after [Fig. 3(d)] applying the first surface voltage pulse. The hydrogen site which appears dark in Fig. 3(c) becomes brighter in Fig. 3(d) as expected from the appearance of the silicon dangling bond after hydrogen desorption. The yield  $Y_d$  for desorbing the hydrogen atom has been obtained by repeating the hydrogen desorption over many different molecules (at  $V_s = -4$  V) and by measuring the mean value  $\tau_d$  of the excitation time  $t_d$  for a given tunnel current  $I$  [ $Y_d = 1/(\tau_d/e)$ ]. A value  $Y_d = (3.4 \pm 0.7) \times 10^{-11}$  has been found which is in good agreement with the value  $Y_d = (2.1 \pm 0.7) \times 10^{-11}$  reported by Stokbro *et al.* [19] for pulses at the same surface voltage.

It is clear from the tunnel current curves in Figs. 3(a) and 3(b) that, after hydrogen desorption, the switching frequencies are significantly increased although the tunnel current levels corresponding to the  $S_1$ ,  $S_2$ , and  $T$  states are unchanged. Quantitative measurements of the  $S_1 \rightarrow S_2$  and

the  $S_1 \rightarrow T$  switching yields for two excitation positions ( $P_1$  and  $P_2$ ) of the STM tip were obtained by using the method described in Ref. [10]. The results in Table I show that, for excitation pulses of  $-3.5$  V, the switching yields are increased after hydrogen desorption by a factor of 3–50 depending on the excitation position and the molecular movement ( $S_1 \rightarrow S_2$  or  $S_1 \rightarrow T$ ). Thus, the consequence of the hydrogen atom desorption can be understood as a lowering of the energy barrier for the switching dynamics ( $S_1 \rightarrow S_2$  or  $S_1 \rightarrow T$ ). Indeed, it is known from the desorption induced by electronic transition mechanism [23] that lowering the energy barrier of the ground state can dramatically increase the yield of the electronic excitation process.

Another interesting result of the hydrogen desorption is that the molecule can now be switched (by applying a pulse voltage at  $V_s = -3.5$  V) into any of the four molecular configurations imaged in Fig. 4. Once the hydrogen atom has been removed, every molecule studied shows the same multistable sites. The  $S_1$  and  $S_2$  states [Figs. 4(a) and 4(c)] are the same as before hydrogen desorption, whereas two new states ( $S_3$  and  $S_4$ ) can be imaged with the STM [Figs. 4(b) and 4(d)]. From the STM images in Figs. 4(b) and 4(d), the molecule in the  $S_3$  and  $S_4$  states appears to lie between the  $S_1$  and  $S_2$  states. Furthermore, these two molecular configurations overlap partially with the silicon dangling bond resulting from the hydrogen desorption. One can expect some interaction between this silicon dangling bond and the molecule, thus explaining the stability of the  $S_3$  and  $S_4$  states after hydrogen desorption under these imaging conditions ( $V_s = -2$  V). The most stable configuration of the  $S_3$  ( $S_4$ ) state deduced from DFT calculations is shown in Fig. 4(h) [Fig. 4(i)]. The corresponding calculated local density of states (integrated over a window of energy from  $-2$  V to the Fermi energy) in Fig. 4(g) is in good agreement with the experimental STM topography in Fig. 4(f). In the tunnel current curves in Figs. 3(a) and 3(b), there are no specific current levels corresponding to the  $S_3$  and  $S_4$  states when the pulse voltage is applied at  $V_s = -4$  V; only  $S_1$ ,  $S_2$ , and  $T$  are seen. This is because the electronic excitation is expected to be very efficient when the molecule is located directly under the STM tip (at the  $P_2$  position) and especially when the surface voltage is relatively high ( $-4$  V). However, after a lower voltage pulse ( $V_s = -3$  V) applied at  $P_2$ , the occurrence of the four stable states ( $S_1$  to  $S_4$ ) and the transient states ( $T$ ) can be seen in the tunnel current curve [Fig. 4(e)]. This reveals that, after hydrogen desorption, the transient states ( $T$ ) are coexisting with the four stable states.

TABLE I. Measured values of the  $S_1 \rightarrow S_2$  and the  $S_1 \rightarrow T$  switching yields for two positions ( $P_1$  and  $P_2$ ) of the STM tip at  $V_s = -3.5$  V before and after hydrogen desorption. See Fig. 2 for the description of positions  $P_1$  and  $P_2$ .

$V_s = -3.5$ V	$Y_{S_1 \rightarrow S_2}(P_1)$	$Y_{S_1 \rightarrow T}(P_1)$	$Y_{S_1 \rightarrow S_2}(P_2)$	$Y_{S_1 \rightarrow T}(P_2)$
Before H desorption [7]	$(1.8 \pm 0.5) \times 10^{-9}$	$(1.5 \pm 0.5) \times 10^{-8}$	$(6.9 \pm 0.7) \times 10^{-11}$	$(4.5 \pm 0.6) \times 10^{-11}$
After H desorption	$(5.3 \pm 0.8) \times 10^{-9}$	$(7.0 \pm 0.5) \times 10^{-8}$	$(1.2 \pm 0.2) \times 10^{-9}$	$(2.1 \pm 0.2) \times 10^{-9}$

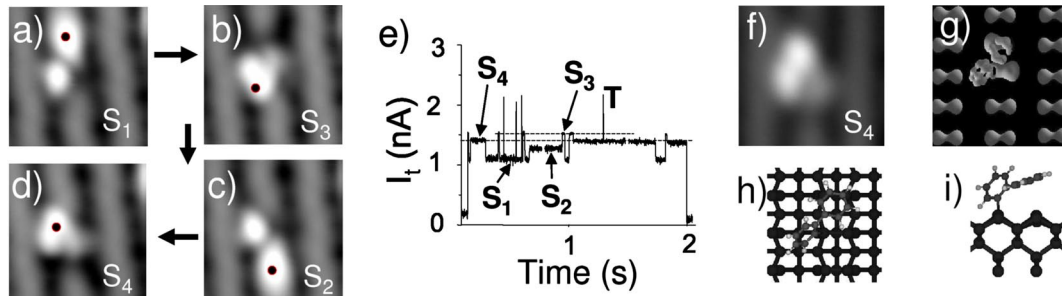


FIG. 4 (color online). ( $23 \text{ \AA} \times 23 \text{ \AA}$ ) STM topographies of the four stable configurations of the biphenyl molecule after H atom desorption. (a),(c) ( $V_s = -2 \text{ V}$ ,  $I = 220 \text{ pA}$ ) depict the  $S_1$  and  $S_2$  configurations, respectively. (b),(d) show the two new stable  $S_3$  and  $S_4$  configurations. The series (a)–(d) (following the arrows) is a succession of molecular manipulations of the multistable molecule using negative surface pulses ( $V_s = -3.0 \text{ V}$ ) applied at the indicated black dots. (e) Tunnel current during a negative bias pulse at  $P_2$  ( $V_s = -3.0 \text{ V}$ ) after hydrogen desorption indicating the coexistence of the four stable states with the transient states ( $T$ ). In addition to the peaks ( $T$  states), plateaus with four different current levels can be observed and are assigned to the four stable states  $S_1$  to  $S_4$ . See Fig. 2 for the description of positions  $P_1$  and  $P_2$ . (f) ( $21 \text{ \AA} \times 21 \text{ \AA}$ ) STM topography of the  $S_4$  state ( $V_s = -2 \text{ V}$ ,  $I = 300 \text{ pA}$ ). (g) Calculated local density of states (VASP) of the  $S_4$  state configuration adsorbed on Si(100)-(2  $\times$  1) within an energy window of  $-2 \text{ eV}$  to the Fermi level. (h) Schematic top view and (i) right-side view of  $S_4$  conformation on the Si(100)-(2  $\times$  1) surface (see Fig. 1 for color definition).

Compared to the operation of the bistable molecule [10], where the biphenyl molecule could be switched only between two stable states ( $S_1$  and  $S_2$ ), the operation of the multistable molecule after hydrogen desorption is much more complicated since it can now be switched between four stable positions ( $S_1$ ,  $S_2$ ,  $S_3$ , and  $S_4$ ). So far, we have found the switching of the multistable molecule to be random. An example of a sequence of switching events is shown in Fig. 4.

In conclusion, these results demonstrate that the presence or not of just one hydrogen atom on the surface dramatically modifies the molecular dynamics of the bistable biphenyl molecule. This is revealed by the increased switching yields and the appearance of two additional stable states after the desorption of a hydrogen atom. Furthermore, this leads to the formation of a multistable molecule having four stable states. These results have important consequences. They demonstrate that a precise control of each atom position around the molecule needs to be achieved if a quantitative operation of a molecular device is required. We emphasize that such single atom sensitivity provides very interesting perspectives for engineering the performance of a molecular device. One can expect being able to control, by single atom manipulation, the intrinsic performances of a molecular device (e.g., the switching yield, the number of stable states, or the bifurcation parameters of a multistable molecule). Moreover, quantum properties of a single computing molecule could also be engineered by similar methods [24].

This work is supported by the European RTN network AMMIST (Contract No. HPRN-CT-2002-00299), the European Integrated project PICO-INSIDE (Contract No. FPG-015847), and the ANR project N3M (Contract No. ANR-05-NANO-020-01). We thank the Institut du Développement et des Ressources en Informatique Scientifique (IDRIS)–Orsay, France, for allocation of computer time.

- [1] L. Cai *et al.*, *Nano Lett.* **5**, 2365 (2005).
- [2] D.M. Eigler, C.P. Lutz, and W.E. Rudge, *Nature (London)* **352**, 600 (1991).
- [3] C. Joachim, J.K. Gimzewski, R.R. Schlittler, and C. Chavy, *Phys. Rev. Lett.* **74**, 2102 (1995).
- [4] G. Dujardin *et al.*, *Phys. Rev. Lett.* **80**, 3085 (1998).
- [5] J. Repp, G. Meyer, M. Stojkovic, A. Gourdon, and Ch. Joachim, *Phys. Rev. Lett.* **94**, 026803 (2005).
- [6] P.A. Sloan and R.E. Palmer, *Nature (London)* **434**, 367 (2005).
- [7] Y. Sainoo, Y. Kim, T. Okawa, T. Komeda, H. Shigekawa, and M. Kawai, *Phys. Rev. Lett.* **95**, 246102 (2005).
- [8] X.H. Qiu, G.V. Nazin, and W. Ho, *Phys. Rev. Lett.* **95**, 166103 (2005).
- [9] M. Di Ventra, S.T. Pantelides, and N.D. Lang, *Phys. Rev. Lett.* **84**, 979 (2000).
- [10] M. Lastapis *et al.*, *Science* **308**, 1000 (2005).
- [11] D. Riedel *et al.*, *Phys. Rev. B* **69**, 121301 (2004).
- [12] A.J. Mayne *et al.*, *Phys. Rev. B* **69**, 045409 (2004).
- [13] G. Kresse and J. Hafner, *Phys. Rev. B* **47**, 558 (1993); **49**, 14251 (1994).
- [14] G. Kresse and J. Furthmüller, *Comput. Mater. Sci.* **6**, 15 (1996).
- [15] G. Kresse and J. Furthmüller, *Phys. Rev. B* **54**, 11169 (1996).
- [16] M. Mamatkulov *et al.*, *Phys. Rev. B* **73**, 035321 (2006).
- [17] J. Tersoff and D.R. Hamann, *Phys. Rev. B* **31**, 805 (1985).
- [18] R.A. Wolkow, G.P. Lopinski, and D.J. Moffatt, *Surf. Sci.* **416**, L1107 (1998).
- [19] K. Stokbro *et al.*, *Phys. Rev. Lett.* **80**, 2618 (1998).
- [20] C. Thirstrup, M. Sakurai, T. Nakayama, and M. Aono, *Surf. Sci.* **411**, 203 (1998).
- [21] T.C. Shen *et al.*, *Science* **268**, 1590 (1995).
- [22] L. Soukiassian, A.J. Mayne, M. Carbone, and G. Dujardin, *Phys. Rev. B* **68**, 035303 (2003).
- [23] G. Comtet and G. Dujardin, *Surf. Sci.* **593**, 256 (2005).
- [24] J. Fiurasek, N.J. Cerf, I. Duchemin, and C. Joachim, *Physica (Amsterdam)* **24E**, 161 (2004).